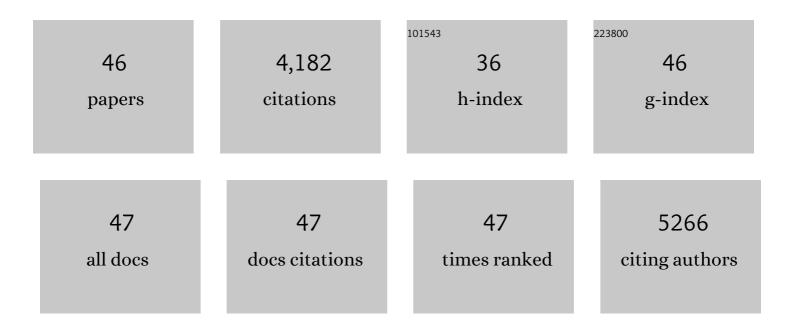
## Shouwei Zhang

List of Publications by Year in descending order

Source: https://exaly.com/author-pdf/9586425/publications.pdf Version: 2024-02-01



#	Article	IF	CITATIONS
1	In Situ Synthesis of Water-Soluble Magnetic Graphitic Carbon Nitride Photocatalyst and Its Synergistic Catalytic Performance. ACS Applied Materials & Interfaces, 2013, 5, 12735-12743.	8.0	290
2	Strongly Coupled gâ€C <sub>3</sub> N <sub>4</sub> Nanosheetsâ€Co <sub>3</sub> O <sub>4</sub> Quantum Dots as 2D/0D Heterostructure Composite for Peroxymonosulfate Activation. Small, 2018, 14, e1801353.	10.0	284
3	Formation of Fe <sub>3</sub> O <sub>4</sub> @MnO <sub>2</sub> ball-in-ball hollow spheres as a high performance catalyst with enhanced catalytic performances. Journal of Materials Chemistry A, 2016, 4, 1414-1422.	10.3	248
4	Constructing electrostatic self-assembled 2D/2D ultra-thin ZnIn2S4/protonated g-C3N4 heterojunctions for excellent photocatalytic performance under visible light. Applied Catalysis B: Environmental, 2019, 256, 117862.	20.2	185
5	One-pot Synthesis of CdS Irregular Nanospheres Hybridized with Oxygen-Incorporated Defect-Rich MoS <sub>2</sub> Ultrathin Nanosheets for Efficient Photocatalytic Hydrogen Evolution. ACS Applied Materials & Interfaces, 2017, 9, 23635-23646.	8.0	178
6	Construction of dual defect mediated Z-scheme photocatalysts for enhanced photocatalytic hydrogen evolution. Applied Catalysis B: Environmental, 2019, 245, 399-409.	20.2	174
7	Engineering of Z-scheme 2D/3D architectures with Ni(OH)2 on 3D porous g-C3N4 for efficiently photocatalytic H2 evolution. Applied Catalysis B: Environmental, 2019, 258, 117997.	20.2	164
8	Ultrathin g-C <sub>3</sub> N <sub>4</sub> nanosheets coupled with amorphous Cu-doped FeOOH nanoclusters as 2D/0D heterogeneous catalysts for water remediation. Environmental Science: Nano, 2018, 5, 1179-1190.	4.3	156
9	Polyaniline nanorods dotted on graphene oxide nanosheets as a novel super adsorbent for Cr(vi). Dalton Transactions, 2013, 42, 7854.	3.3	151
10	Unexpected ultrafast and high adsorption capacity of oxygen vacancy-rich WO <sub>x</sub> /C nanowire networks for aqueous Pb <sup>2+</sup> and methylene blue removal. Journal of Materials Chemistry A, 2017, 5, 15913-15922.	10.3	150
11	Efficient enrichment of uranium(vi) on amidoximated magnetite/graphene oxide composites. RSC Advances, 2013, 3, 18952.	3.6	147
12	Rice husks as a sustainable silica source for hierarchical flower-like metal silicate architectures assembled into ultrathin nanosheets for adsorption and catalysis. Journal of Hazardous Materials, 2017, 321, 92-102.	12.4	136
13	Amidoxime-functionalized magnetic mesoporous silica for selective sorption of U( <scp>vi</scp> ). RSC Advances, 2014, 4, 32710.	3.6	135
14	Superior adsorption capacity of hierarchical iron oxide@magnesium silicate magnetic nanorods for fast removal of organic pollutants from aqueous solution. Journal of Materials Chemistry A, 2013, 1, 11691.	10.3	133
15	MOF-derived CoN/N-C@SiO2 yolk-shell nanoreactor with dual active sites for highly efficient catalytic advanced oxidation processes. Chemical Engineering Journal, 2020, 381, 122670.	12.7	127
16	Hybrid 0D–2D Nanoheterostructures: In Situ Growth of Amorphous Silver Silicates Dots on g-C <sub>3</sub> N <sub>4</sub> Nanosheets for Full-Spectrum Photocatalysis. ACS Applied Materials & Interfaces, 2016, 8, 35138-35149.	8.0	111
17	Efficient removal of metal contaminants by EDTA modified MOF from aqueous solutions. Journal of Colloid and Interface Science, 2019, 555, 403-412.	9.4	104
18	Three-Dimensional Hierarchical g-C <sub>3</sub> N <sub>4</sub> Architectures Assembled by Ultrathin Self-Doped Nanosheets: Extremely Facile Hexamethylenetetramine Activation and Superior Photocatalytic Hydrogen Evolution. ACS Applied Materials & Interfaces, 2019, 11, 2050-2059.	8.0	103

SHOUWEI ZHANG

#	Article	IF	CITATIONS
19	Fabrication of Fe/Fe <sub>3</sub> C@porous carbon sheets from biomass and their application for simultaneous reduction and adsorption of uranium( <scp>vi</scp> ) from solution. Inorganic Chemistry Frontiers, 2014, 1, 641.	6.0	86
20	Hierarchical nanocomposites of polyaniline nanorods arrays on graphitic carbon nitride sheets with synergistic effect for photocatalysis. Catalysis Today, 2014, 224, 114-121.	4.4	73
21	Amidoxime-Functionalized Hollow Carbon Spheres for Efficient Removal of Uranium from Wastewater. ACS Sustainable Chemistry and Engineering, 2019, 7, 10800-10807.	6.7	70
22	Visibleâ€Light Photocatalytic Degradation of Methylene Blue Using SnO <sub>2</sub> /αâ€Fe <sub>2</sub> O <sub>3</sub> Hierarchical Nanoheterostructures. ChemPlusChem, 2013, 78, 192-199.	2.8	69
23	Surface functional groups and defects on carbon nanotubes affect adsorption–desorption hysteresis of metal cations and oxoanions in water. Environmental Science: Nano, 2014, 1, 488-495.	4.3	69
24	Hierarchically grown CdS/α-Fe2O3 heterojunction nanocomposites with enhanced visible-light-driven photocatalytic performance. Dalton Transactions, 2013, 42, 13417.	3.3	65
25	Synthesis of TiO <sub>2</sub> Nanoparticles on Plasma-Treated Carbon Nanotubes and Its Application in Photoanodes of Dye-Sensitized Solar Cells. Journal of Physical Chemistry C, 2011, 115, 22025-22034.	3.1	62
26	Sandwich-like P-doped h-BN/ZnIn2S4 nanocomposite with direct Z-scheme heterojunction for efficient photocatalytic H2 and H2O2 evolution. Chemical Engineering Journal, 2022, 442, 136151.	12.7	62
27	Constructing highly dispersed 0D Co3S4 quantum dots/2D g-C3N4 nanosheets nanocomposites for excellent photocatalytic performance. Science Bulletin, 2019, 64, 1510-1517.	9.0	58
28	Constructing the novel ultrafine amorphous iron oxyhydroxide/g-C3N4 nanosheets heterojunctions for highly improved photocatalytic performance. Scientific Reports, 2017, 7, 8686.	3.3	53
29	ZnO@CdS Core-Shell Heterostructures: Fabrication, Enhanced Photocatalytic, and Photoelectrochemical Performance. Nanoscale Research Letters, 2016, 11, 205.	5.7	51
30	One-pot hydrothermal synthesis of CdS decorated CuS microflower-like structures for enhanced photocatalytic properties. Scientific Reports, 2017, 7, 3877.	3.3	51
31	Reduced interfacial recombination in dye-sensitized solar cells assisted with NiO:Eu3+,Tb3+ coated TiO2 film. Scientific Reports, 2016, 6, 31123.	3.3	49
32	Metal organic framework derived heteroatoms and cyano ( C N) group co-decorated porous g-C3N4 nanosheets for improved photocatalytic H2 evolution and uranium(VI) reduction. Journal of Colloid and Interface Science, 2020, 570, 125-134.	9.4	44
33	Hierarchical flowerlike metal/metal oxide nanostructures derived from layered double hydroxides for catalysis and gas sensing. Journal of Materials Chemistry A, 2017, 5, 23999-24010.	10.3	43
34	Surface Area- and Structure-Dependent Effects of LDH for Highly Efficient Dye Removal. ACS Sustainable Chemistry and Engineering, 2019, 7, 905-915.	6.7	39
35	Cellulose Fibers Constructed Convenient Recyclable 3D Graphene-Formicary-like δ-Bi <sub>2</sub> O <sub>3</sub> Aerogels for the Selective Capture of Iodide. ACS Applied Materials & Interfaces, 2017, 9, 20554-20560.	8.0	38
36	In-situ synthesis of amorphous silver silicate/carbonate composites for selective visible-light photocatalytic decomposition. Scientific Reports, 2017, 7, 15001.	3.3	37

SHOUWEI ZHANG

#	Article	IF	CITATIONS
37	Hierarchical multi-active component yolk-shell nanoreactors as highly active peroxymonosulfate activator for ciprofloxacin degradation. Journal of Colloid and Interface Science, 2022, 605, 766-778.	9.4	37
38	Dopant and Defect Doubly Modified CeO <sub>2</sub> /g-C <sub>3</sub> N <sub>4</sub> Nanosheets as 0D/2D Z-Scheme Heterojunctions for Photocatalytic Hydrogen Evolution: Experimental and Density Functional Theory Studies. ACS Sustainable Chemistry and Engineering, 2021, 9, 11479-11492.	6.7	36
39	Noble metal-free core-shell CdS/iron phthalocyanine Z-scheme photocatalyst for enhancing photocatalytic hydrogen evolution. Journal of Materials Science and Technology, 2022, 115, 199-207.	10.7	25
40	Fabrication of Hierarchical ZnO@NiO Core–Shell Heterostructures for Improved Photocatalytic Performance. Nanoscale Research Letters, 2018, 13, 260.	5.7	22
41	Construction of 3DOM Carbon Nitrides with Quasiâ€Honeycomb Structures for Efficient Photocatalytic H <sub>2</sub> Production. ChemCatChem, 2018, 10, 5656-5664.	3.7	21
42	Activating and optimizing activity of CdS@g-C3N4 heterojunction for photocatalytic hydrogen evolution through the synergistic effect of phosphorus doping and defects. Journal of Alloys and Compounds, 2020, 834, 155201.	5.5	21
43	Improving the photovoltaic performance of dye sensitized solar cells based on a hierarchical structure with up/down converters. RSC Advances, 2016, 6, 11880-11887.	3.6	15
44	Construction of cobalt nanoparticles decorated intertwined N-doped carbon nanotube clusters with dual active sites for highly effective 4-nitrophenol reduction. Journal of Alloys and Compounds, 2021, 858, 158287.	5.5	5
45	Enhanced Dye-Sensitized Solar Cell Efficiency by Insertion of a H <sub>3</sub> PW <sub>12</sub> O <sub>40</sub> Layer Between the Transparent Conductive Oxide Layer and the Compact TiO <sub>2</sub> Layer. Science of Advanced Materials, 2018, 10, 867-871.	0.7	4
46	New Properties of Twoâ€Dimensional Materials: Highly Effective Thermal Catalytic Degradation Activity. ChemistrySelect, 2018, 3, 10133-10138.	1.5	1